ECS Solid State Letters, **4** (1) M1-M4 (2015)
2162-8742/2015/4(1)/M1/4/$31.00 © The Electrochemical Society

Plasma Treatment of Carbon Nanofibers Using an Anode Layer Ion Source for High-Performance Electrochemical Capacitors

Yu-Jin Lee,[a] Do-Geun Kim,[b,z] and Hyo-Jin Ahn[a,z]

[a]*Department of Materials Science and Engineering, Seoul National University of Science and Technology, Seoul 139-743, Korea*
[b]*Surface Technology Division, Korea Institute of Materials Science, Gyeongnam 642-831, Korea*

We synthesized carbon nanofibers(CNFs) by electrospinning and then activated their surface states via plasma treatment with an anode layer ion source. We studied the effects of various treatment times—0, 400, 800, and 1200 seconds—in order to identify the optimum conditions for plasma treatment. We investigated the morphological and structural properties, and the chemical composition of the CNFs using scanning electron microscopy, transmission electron microscopy, Raman spectroscopy, Fourier transform infrared spectroscopy, and X-ray photoelectron spectroscopy. The activated CNFs—plasma-treated for 1200s—exhibited excellent capacitance(∼173.25 F/g at 5 mV/s), superb cycling stability(∼92.59%), and the highest energy density(∼6.81 Wh/kg) among the different samples produced.
 [DOI: 10.1149/2.0061501ssl]

Manuscript submitted October 7, 2014; revised manuscript received November 7, 2014. Published November 21, 2014.

Electrochemical capacitors (ECs), because of their high power density, fast charge-discharge rates, and long cycle life, are one of the most promising energy storage systems for a number of applications such as in hybrid electric vehicles, portable electronic devices, and flashlights.[1] In general, ECs can be divided into two categories depending on the charge storage mechanism and the active materials used, viz. pseudocapacitors and electrical double-layer capacitors (EDLCs). In pseudocapacitors, the electrode materials (e.g., transition metal oxides (RuO_2, MnO_x, and CoO_x) and conducting polymers (PEDOT, PPy, and PANI)) undergo a reversible faradaic process at the electrode/electrolyte interface during charge storage. EDLCs operate via a non-faradaic process whereby electrostatic forces adsorb solvated ions along the electrode/electrolyte surface by forming an electrical double-layer. Carbon-based materials (e.g., activated carbons, carbon nanotubes (CNTs), or carbon nanofibers (CNFs)) are usually chosen for EDLC electrodes because of their high specific surface area and relatively low cost. Moreover, EDLCs are more stable under cycling than pseudocapacitors because EDLCs do not participate in redox reactions; hence the electrodes of the latter suffer little deterioration. In spite of these advantages, the low energy density in EDLCs is a serious drawback.[2] One strategy to overcome this problem is to modify the functional groups on the surface of the carbon materials using wet-chemical etching. On the other hand, dry etching processes such as plasma treatment offer the dual benefits of simplicity and non-toxicity. Although the surface modification of carbon materials in a plasma has been reported, the potential in this context of linear anode-layer ion source (ALIS) treatment has not been investigated so far. The ALIS in our study is based on drift-type linear ion sources. Electrons are trapped in the mixed electric and magnetic fields of an ionized gas and ions are emitted after being accelerated in the anode layer. This ALIS can generate linear ions at a distance of 3 m that are accelerated up to energies of several keV at the anode surface.[3] This setup offers control of the ion beam energy as well as several advantages over existing plasma treatments: (1) the plasma treatment time is short, (2) the chemical states and morphology of the surface are easily controlled, (3) mass production is possible using roll to roll systems.

We therefore synthesized CNFs by electrospinning and then employed an ALIS to activate their surface to prepare them for use in high-performance ECs.

Experimental

We synthesized conventional CNFs by electrospinning. Polyacrylonitrile (PAN, Aldrich) and polyvinylpyrrolidone (PVP, Aldrich) were dissolved in *N,N*-dimethylformamide (DMF, Aldrich). The solution was stirred for 5 h at room temperature and was then loaded into a plastic syringe equipped with a 23-gauge stainless steel needle. The distance between the needle tip and the collector, the applied voltage, and the feeding rate were fixed at ∼15 cm, 13 kV, and 0.03 mL/h, respectively. The as-spun samples were heat-treated at 230°C for 2 h in air and then carbonized at 800°C for 2 h in a N_2 atmosphere. The resultant CNFs were activated by plasma treatment using an ALIS in a vacuum chamber evacuated to 5.0×10^{-5} Torr using rotary and high-vacuum pumps. A 450-mm-wide ALIS was used under a mixture of O_2 and H_2 mixed with Ar gasses, at a working pressure of 3.9 mTorr. The ion flux was ∼0.319 mA/cm^2. About 40% of the applied discharge voltage (1.5 kV), that is, an average energy of ∼600 eV, was applied to the samples. Plasma treatments were performed for 0, 400, 800, or 1200 s (referred to herein as conventional CNFs, ACNFs-400, ACNFs-800, and ACNFs-1200), to investigate the optimum conditions for CNF surface treatments.

The morphological and structural properties of the samples were investigated using a field emission scanning electron microscope (FE-SEM; Hitachi S-4800) and a transmission electron microscope (TEM; Tecnai G,[2] KBSI Gwangju center). The surface chemical composition of the samples was characterized by Raman spectroscopy (SENTERRA Raman) with a 532 nm Ar ion laser source; Fourier transform infrared spectroscopy (FT-IR; Bruker IFS-66/S) using the KBr disc method with wavenumbers ranging from 4000 to 400 cm^{-1}, and X-ray photoelectron spectroscopy (XPS; ESCALAB 250). The electrochemical performance of the samples was evaluated in 0.5 M H_2SO_4 using a potentiostat/galvanostat (PGST302N, Eco Chemie) in a conventional three-electrode system consisting of a working electrode, a reference electrode, and a counter electrode. For the working electrode, the ink was prepared by mixing active materials, acetylene black, and polyvinylidene fluoride (PVDF) binder in a weight ratio of 7:2:1 in N-methyl-2-pyrrolidinone (NMP). This was then loaded onto the glassy carbon working electrode (CH Instruments), and then dried at 80°C. The mass of the electrode was thereby fixed to 5.28 mg/cm^2. Ag/AgCl (saturated with KCl) and Pt wires were used as reference and counter electrodes, respectively. Cyclic voltammetry (CV) measurements were performed at scan rates between 5 and 200 mV/s in the potential range of 0.0–1.0 V. The capacitance of the electrodes was calculated using the following equation:[1]

$$C = (q_a + q_c)/(2m \times \Delta V)$$

where q_a and q_c are the charges of the anodic and cathodic region, respectively, m is the mass of active material (g), and ΔV is the potential range of the CV measurements (V). The galvanostatic charge/discharge tests were performed with a battery cycler (WonATech Corp. Korea) with a two-electrode system, between 0 and 1.0 V at current densities ranging from 0.5 to 10 A/g in a 6 M KOH

[z]E-mail: dogeunkim@kims.re.kr; hjahn@seoultech.ac.kr

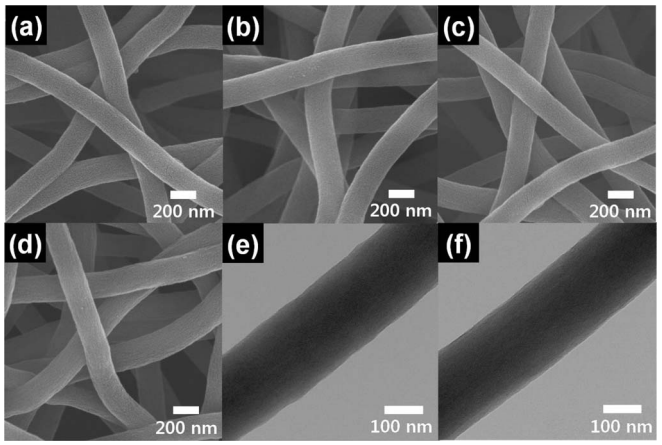

Figure 1. SEM images obtained from (a) the conventional CNFs, (b) ACNFs-400, (c) ACNFs-800 and (d) ACNFs-1200. TEM images obtained from (e) the conventional CNFs and (f) ACNFs-1200.

electrolyte. The paste was loaded onto Ni foam as the current collector. The total mass of the electrode was fixed at ∼4.03 mg/cm^2. The performance of the sample was evaluated over 5,000 cycles at a current density of 1 A/g. The energy and power densities were measured at discharge current densities ranging from 0.2 to 10 A/g. Electrochemical impedance spectroscopy (EIS) measurements were performed with a two-electrode system for frequencies ranging from 100 kHz to 10 mHz under an AC potential of 10 mV.

Results and Discussion

Figures 1a–1d show FESEM images of conventional CNFs, ACNFs-400, ACNFs-800, and ACNFs-1200, which are ∼187–216 nm, ∼185–215 nm, ∼176–213 nm, and ∼174–206 nm in diameter, respectively. The diameters of the CNFs are slightly reduced after plasma treatment due to surface etching effects; however, for all samples, a smooth CNF surface and uniform CNF morphology are observed. In Figures 1e and 1f, furthermore, a uniform bright-gray contrast is observed in the TEM images obtained from conventional CNFs and ACNFs-1200, indicating that these consist of a single phase, and that no macro-pores are generated during the plasma treatment. These results therefore demonstrate that the plasma treatment does not lead to any dramatic changes in surface morphology.

Figure 2a shows the Raman spectra of the samples for wavenumbers ranging from 600 to 2200 cm^{-1}. Generally, in these types of samples, the G-band reflects an ordered structure corresponding to in-plane sp^2 vibrations of the graphite lattice (E_{2g} mode), which the D-band is related to the disordered structure induced by defects (A_{1g} mode). The D- to G-band intensity ratio (I_D/I_G) can be used to quantify structural imperfections, such as changes in the chemical bonding or an increase in the number of defects on the CNFs.[4] From Figure 2a, the I_D/I_G ratios gradually increase with the plasma treatment time, with 0.96, 0.97, 0.98, and 1.00 measured for the conventional CNFs, ACNFs-400, ACNFs-800, and ACNFs-1200, respectively. It should be noted that for the ACNFs-1200, two of the weaker peaks become broad, which can be explained by an increased number of structural defects on the CNF surface caused by prolonged ion bombardment during the plasma treatment.[4] FT-IR spectra were recorded, as shown in Figure 2b, to gather further information on the functional groups on the surface of the samples. The peaks observed at ∼3400 cm^{-1} are assigned to O-H stretching due to surface-adsorbed moisture.[5] The strong peaks at ∼1560 cm^{-1} and ∼1218 cm^{-1} are due to asymmetric COO^- stretching in carboxylate groups and C-O stretching in C-O groups, respectively.[5,6] Interestingly, the peaks related to aliphatic C-H stretching at 2850 cm^{-1} and 2920 cm^{-1}, observed in the spectrum for the conventional CNFs disappear as the plasma treatment time increases.[7] Thus, for ACNFs-1200, no peaks corresponding to aliphatic C-H stretching are observed. As will be discussed later, this property of the CNFs directly affects the performance of EDLCs. XPS measurements were carried out in order to examine the chemical bonding states of the CNF surfaces in more detail and to quantify oxygen-containing functional groups before and after plasma treatment. Figures 2c–2d show the C1s XPS spectra obtained from the surface of conventional CNFs and ACNFs-1200. The C1s spectra can be decomposed into four peaks at ∼284.5, ∼286.0, ∼287.3, and ∼288.9 eV, corresponding to C-C, C-O, C = O, and COO^- groups, respectively.[8,9] After plasma treatment, the proportion of graphitic carbon (peak 1) decreases from 63.0% to 56.4%, while the peaks assigned to carbon-oxygen functional groups (peaks 2–4) become more intense, from 17.3%, 11.1%, and 8.4% to 20.2%, 13.0%,

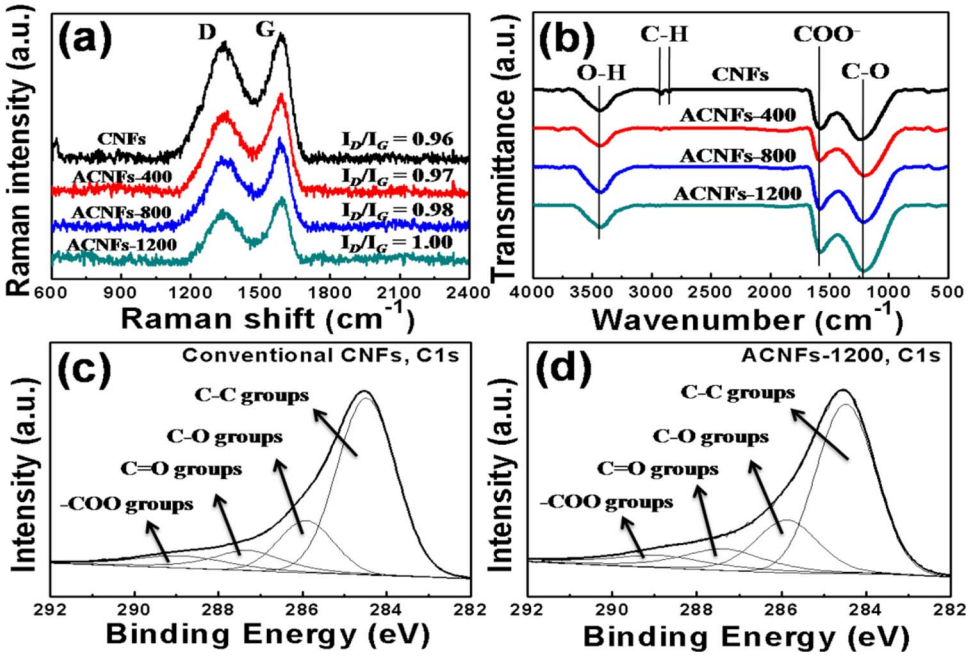

Figure 2. (a) Raman and (b) FTIR spectra obtained from all the samples. XPS results of C1s spectra of (c) the conventional CNFs and (d) ACNFs-1200.

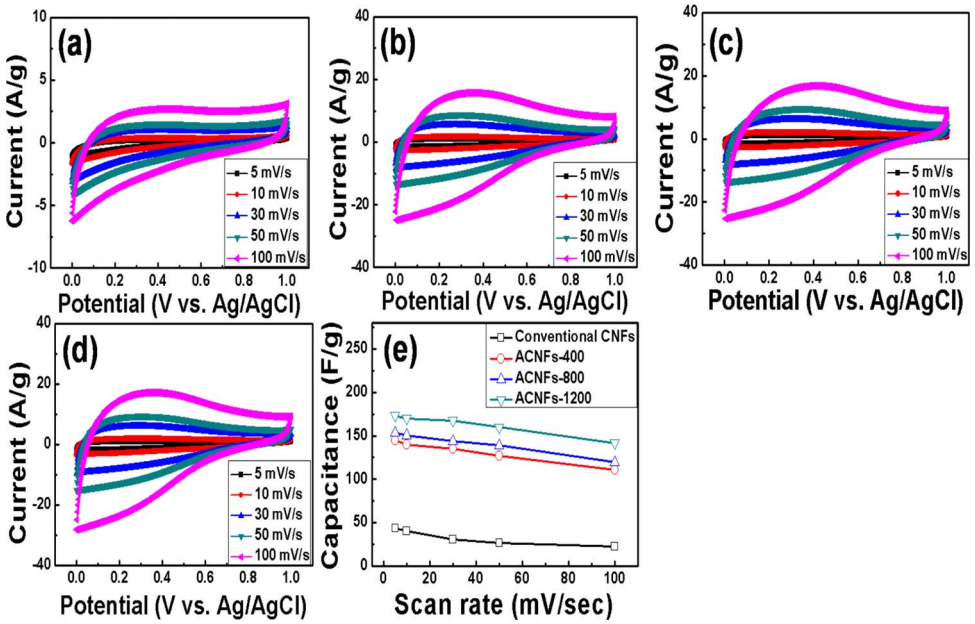

Figure 3. Cyclic voltammograms of (a) the conventional CNFs, (b) ACNFs-400, (c) ACNFs-800, and (d) ACNFs-1200 at scan rate from 2 mV/s to 100 mV/s in the potential range 0.0–1.0 V. (e) Capacitances of all the samples at different scan rates derived from their CVs.

and 10.3% of the integrated intensity, respectively. These results imply that the surface states are activated by the oxygen contained in the inserted gas and that the plasma treatment breaks the chemical bonds on the edges of the CNF surfaces.

Figures 3a–3d shows the cyclic voltammograms measured for all the samples, which were recorded using a three-electrode system at scan rates from 5 to 100 mV/s in the potential range of 0.0–1.0 V. The capacitances of the conventional CNFs, ACNFs-400, ACNFs-800, and ACNFs-1200 at 5 mV/s are ∼43.3, ∼144.7, ∼153.5, and ∼173.2 F/g, respectively. It can be seen that the capacitance of the ACNFs-1200 is ∼4 times higher than that of the conventional CNFs. Also, as shown in Figure 3d, the CV spectra of all the plasma-treated samples exhibit pseudocapacitive behavior around ∼0.4 V, implying that redox reactions occur. Finally, Figure 3e shows the high-rate performances of all the samples as obtained from the spectra in Figures 3a–3d. In particular, the capacitance retention of the ACNFs-1200 is the best (∼81.80%) among all the samples, highlighting its superior high-rate performance.

To further investigate the electrochemical performance before and after plasma treatment, the galvanostatic charge/discharge properties of the conventional CNFs and ACNFs-1200 were characterized in a symmetric two-electrode system with a 6 M KOH electrolyte. Figure 4a shows the charge/discharge behaviors of the ACNFs-1200 measured at current densities ranging from 0.2 to 10 A/g.

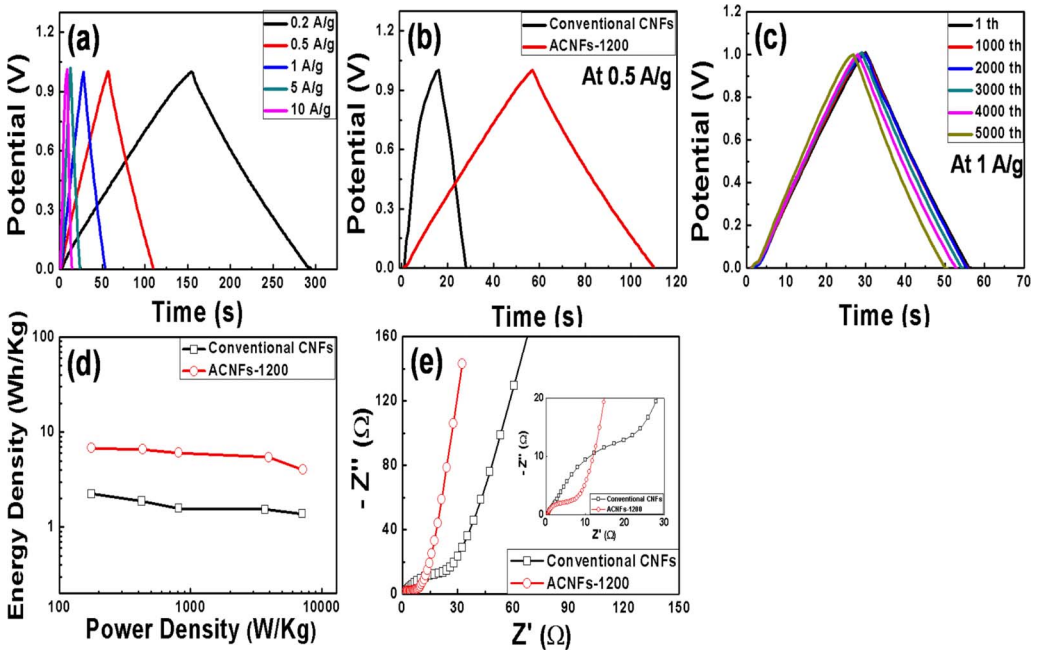

Figure 4. (a) Galvanostatic charge/discharge curves of ACNFs-1200 with different current densities ranging from 0.2 A/g to 10 A/g using symmetric two-electrode cells. (b) A comparison of the galvanostatic charge/discharge curves of the conventional CNFs and ACNFs-1200 at 0.5 A/g. (c) Cycle performances of ACNFs-1200 during 5000 cycles at the current density of 1.0 A/g. (d) A Ragone plot of the conventional CNFs and ACNFs-1200 in 6 M KOH solution. (e) Nyquist plots of the conventional CNFs and ACNFs-1200 recorded from 100 kHz to 10 mHz at an AC potential of 10 mV.

The charge/discharge curves are almost linear and symmetric, implying ideal capacitive behavior. Furthermore, the discharge time of the ACNFs-1200 at a current density of 0.5 A/g is 54 s, which is ∼4.15 times longer than for conventional CNFs (13 s), as shown in Figure 4b. Figure 4c shows the cycling stability of the ACNFs-1200 electrode at a current density of 1 A/g, with ∼92.59% of the initial capacitance retained after 5,000 cycles, emphasizing its excellent cycling stability. In order to demonstrate the operational performance of the electrode, the energy density (E, Wh/kg) and power density (P, W/kg) were obtained from the galvanostatic discharge curves, and Ragone charts were produced at discharge current densities ranging from 0.2 to 10 A/g, as shown in Figure 4d. Specifically, the energy and power densities were calculated using the following equation:[10]

$$E = C \cdot (\Delta V)^2/8, \quad P = E/\Delta t$$

where C is the specific gravimetric capacitance (F/g), ΔV is the discharge voltage excluding the initial voltage drop (V), and Δt is the discharge time (s). Thereby, the maximum energy density of ∼6.81 Wh/kg (power density of ∼7.2 kW/kg) is obtained for the ACNFs-1200, ∼3.04 times higher than for the conventional CNFs. Figure 4e shows the Nyquist plots obtained for the conventional CNFs and ACNFs-1200. In the high frequency region, the semicircles indicate charge transfer resistance (R_{ct}) at the electrode/electrolyte interface. The ACNFs-1200 has a lower R_{ct} than the conventional CNFs. In the low-frequency range, the steeper gradient obtained for the ACNFs-1200 along the imaginary axis implies improved ion diffusion within the ACNFs, probably due to a greater number of oxygen functional groups. Thus, after the plasma treatment, the improved performance of the ACNFs-1200 is attributed to the synergistic effects of, on the one hand, the pseudocapacitive behavior arising from the oxygen-containing functional groups formed on the CNF surface, and on the other, the increased ion adsorption stemming from the improved wettability of the CNF in the aqueous electrolyte. These results therefore show that CNF surface activation affords high EC performance and highlight the promise of ALIS-based plasma treatment for the chemical activation of CNF surfaces.

Conclusions

CNFs were synthesized by electrospinning and activated using an ALIS. Among the samples produced using different plasma treatment times, the ACNFs-1200 (treated for 1200 s) showed a superior capacitance (∼173.25 F/g at 5 mV/s), a good high-rate performance (∼81.80%), excellent cycling stability (∼92.59%), and a high energy density (∼6.81 Wh/kg). The improved electrochemical properties of the ACNFs-1200 after plasma treatment are attributed to an increase in the number of oxygen-containing functional groups on the surface of the CNFs, and to the enhanced wettability of the latter in the aqueous electrolyte.

Acknowledgment

This research was supported by Basic Science Research Program through the National Research Foundation of Korea(NRF) funded by the Ministry of Education, Science and Technology(2012-007444).

References

1. G.-H. An and H.-J. Ahn, *Electrochem. Solid-State Lett.*, **2**, M33 (2013).
2. G. Yu, X. Xie, L. Pan, Z. Bao, and Y. Cui, *Nano Energy*, **2**, 213 (2013).
3. S. Lee, J.-K. Kim, and D.-G. Kim, *Rev. Sci. Instrum.*, **83**, 02B703 (2012).
4. A. Gohel, K. C. Chin, Y. W. Zhu, C. H. Sow, and A. T. S. Wee, *Carbon*, **43**, 2530 (2005).
5. M. Zhi, A. Manivannan, F. Meng, and N. Wu, *J. Power Sources*, **208**, 345 (2012).
6. C. Velasco-Santos, A. L. Martinez-Hernandez, M. Lozada-Cassou, A. Alvarez-Castillo, and V. M. Castano, *Nanotechnology*, **13**, 495 (2002).
7. T. Mitome, Y. Uchida, Y. Egashira, and N. Nishiyama, *Colloids and Surfaces A: Physicochem. Eng. Aspects*, **449**, 51 (2014).
8. A. P. Terzyk, *Colloids and Surfaces A: Physicochem. Eng. Aspects*, **177**, 23 (2001).
9. Z. R. Yue, W. Jiang, L. Wang, S. D. Gardner, and C. U. Pittman Jr., *Carbon*, **37**, 1785 (1999).
10. X. Yang, L. Zhang, F. Zhang, T. Zhang, Y. Huang, and Y. Chen, *Carbon*, **72**, 381 (2014).